A Preliminary Examination of Variability Due to Build Location and Powder Feedstock in Additive Manufacture of Inconel 718 using Laser-Based Powder Bed Fusion

David B. Saint John[*], Sanjay B. Joshi[*], Timothy W. Simpson[*],
Meng Qu[†], John David Rowatt[†], and Yucun Lou[†]

[*]Industrial & Manufacturing Engineering, Penn State University, University Park, PA 16802
[†]Mechanical & Materials Science, Schlumberger-Doll Research, Cambridge, MA 02139

Abstract

The production of metallic parts by additive manufacturing (AM) is of significant interest to industry, but in the absence of standards, practical design considerations for manufacturing engineers are not widely known. Within the context of powder bed fusion (PBF), many unknowns persist regarding variations in part quality due to part location on the build plate, process consistency, feedstock supplier, and machine manufacturer. In this paper, we investigate the mechanical property variance across the build platform and document the successful use of feedstock powders obtained from several suppliers for the manufacture of Inconel 718 tensile and Charpy specimens, built on an EOS M280 laser-based powder bed fusion system. Particular emphasis is placed on describing the manufacturing process design challenges encountered even for simple geometries. While many advocate that complexity is free when using AM, we find that AM can lead to expensive build failures given the current state of manufacturing process knowledge and that design for additive manufacture is required for successful application of AM techniques.

1. Introduction

Additive Manufacturing (AM) of metallic parts offers much promise for the production of highly engineered components, but the relative youth of these processes means that they still contain many unknowns (Gao et al., 2015). In particular, concerns remain regarding the strength and microstructure of as-built parts (Frasier, 2014; Nassar et al., 2014), the associated routes for post-processing methodology including heat treatment and machining (Gibson et al, 2010; Gratton, 2012), and the relative variance in a build due to variation in powder supplier, handling, size distribution, and composition (Gibson et al, 2010; Spierings et al, 2011, Gao et al, 2015).

These concerns are present within a given material class as well as for specific equipment manufacturers. For instance, initial heat treatment studies of 17-4 material from EOS GmbH were found to exhibit anomalous responses to aging heat treatments, later associated with the method of manufacture of the feedstock powder (Gratton, 2012). Moreover, process consistency across equipment manufacturers has not been demonstrated either, and it creates another source of variation in metallic parts produced using AM (Frazier, 2014). Machine-to-machine and process-to-process variation remains a critical source of uncertainty in additive manufacturing of metallic components. This is hindering industry adoption, challenging standards development, and making part qualification and certification expensive and time-consuming.

Given the wide range of materials and processes available (Frasier, 2014), in this study we narrow our focus to the production of Inconel 718 parts manufactured using a powder bed fusion (PBF) process. Inconel 718 was chosen because of its widespread use in both airspace and oilfield applications and its availability in a PBF process. Despite the nominal similarity in materials, the exact compositions, heat treatments, and final microstructures are application specific (Bhavsar et al, 2001; Debarbadillo and Mannan, 2012) and some baseline understanding of the available Inconel 718 PBF material will support further application-specific study. It is expected that further control of beam pathing and processing conditions may lead to deliberate tailoring of the as-built microstructure, and preliminary studies have demonstrated this with electron beam systems (Morton, et al., 2015).

The next section reviews related work fabricating Inconel 718 parts with powder bed fusion (PBF). We then narrow our scope to investigations with the EOS GmbH direct metal laser sintering (DMLS) powder bed fusion process, which is used for the experimental work described in Section 3. Our results are discussed in Section 4, and closing remarks and future work are offered in Section 5.

2. Additive Manufacturing of Inconel 718

Inconel 718 has been produced using a variety of additive methods in addition to PBF, including electron-beam AM methods and directed energy AM methods (Murr et al, 2012; Zhang et al, 2013). While there are some similarities between any processes in which a material has undergone rapid solidification, it has been shown that the grain size, solidification microstructures, and resulting mechanical properties do vary somewhat among additive processes (Frasier, 2014). While there is prior research (Blackwell, 2005; Zhao et al, 2008; Fulcher and Leigh, 2013; Jia and Gu, 2014; Scott-Emuakpor et al., 2015) regarding the microstructural and mechanical properties of as-built Inconel 718 manufactured via PBF (and related) processes, the detailed manufacturing considerations and limitations are seldom discussed, but any user of metals AM is inherently constrained by the capabilities presented by the equipment manufacturer. In this work, we use an EOS M280 system, which generally (as of writing) constrains a user's ability to see/edit parameters associated with the layer heights and beam settings used. Despite these constraints, the parts produced by the system are typically dense and reports on this process and material have begun to enter the literature (Fulcher and Leigh, 2013).

In light of the previous studies, the objective in this work is to explore the range of variability that can be encountered while laying out and building test specimens for the measurement of the mechanical properties and microstructure of Inconel 718 in an EOS M280 laser-based powder bed fusion AM system. Specifically we focus on two aspects contributing to variability in this particular AM process:

1. Location of the samples on the build plate: The EOS M280 is designed to blow inert gas over the surface of the build region from back to front to remove metal condensates and other melt pool ejecta (so-called 'cross-flow') as shown in Figure 1. It is possible that an inherent front-to-back asymmetry may be introduced into the build area (Ferrar et al, 2012), either due to thermal history variations or the migration of larger particles from exposure events near the

back of the build plate which 'kick' larger particles to the front of the build plate. We seek to determine if mechanical property variations may result from the presence of this cross-flow.
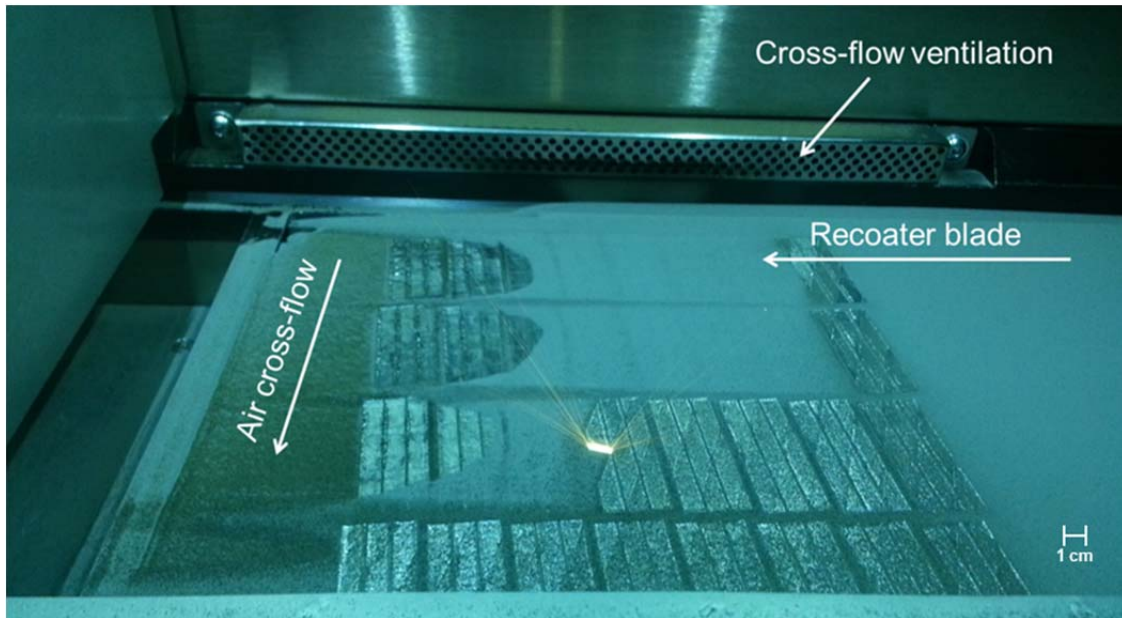

Figure 1: Melt pool ejecta often arise during builds in powder bed fusion and cross-flow ventilation is used to remove these ejected particles from the build

2. <u>Alternative powder feedstocks from different suppliers</u>: Powder feedstock is expensive for PBF, and most equipment manufacturers mandate the use of their powder to ensure proper operation of their equipment. There is strong interest by companies across many industries to use powder feedstocks from different suppliers to reduce cost and increase the powder supplier base, yet *no published studies have examined the impact of variability in material and microstructure properties that arise from using similar yet different powder feedstock*. An issue is whether the standard processing parameters for a given material (e.g., EOS IN718) on a given machine (EOS M280) work well with a comparable powder provided by different suppliers.

While conducting these studies, we encountered several manufacturing challenges during the fabrication of simple tensile and Charpy specimens produced for the assessment of as-built and mechanical properties of Inconel 718. Considerations regarding manufacturability, part layout/build design, and adequate support structures were some of the unplanned challenges that we faced in this work, and they are documented in the paper. These types of manufacturing challenges are often not discussed in the literature, yet they are critical to understand the capabilities and limitations of AM in practical settings. These findings contribute to the body of knowledge for manufacturing process design for PBF, specifically, and AM, in general, and also provide context for microstructural characterization of these materials and guidance for future AM materials characterization efforts.

3. Experimental Procedure

The experimental procedure used in this work is described in this section. Specifically, the equipment set up and operation, test specimen design and build layout, powder feedstock, and post-processing and mechanical testing procedures are detailed as follows.

3.1 Equipment Set Up and Operation

All builds described in this work were fabricated using an EOS M280 laser-based powder bed fusion system (commonly referred to as DMLS by EOS), using the standard processing parameters provided by EOS for producing IN718 parts using a layer height of 40 microns. All recommended processing options for IN718 were maintained as specified in the M280 operator's manual. For instance, a high-speed steel recoater blade and steel build plate were installed, the recirculating flow filter was set to 2.5 Volts, and argon was supplied as the shielding gas. The build chamber was cleaned thoroughly prior to changing the feedstock powder, with all mechanical stages moved to their extreme positions several times during the cleaning process, prior to homing before the initiation of the build process.

3.2. Test Specimen and Build Layout

Blanks for test specimens were built with the expectation that the test specimens would be machined from the blanks. As per ASTM standards E8 and E23, rectilinear blanks for tensile (0.6 cm x 0.6 cm x 5 cm) and Charpy specimens (1.1 cm x 1.1 cm x 5.6 cm) were fabricated and then machined down for mechanical testing. Comparable test specimens were also fabricated from wrought Inconel 718 to provide a benchmark for comparison.

To assess the possible thermal variability that may arise from cross-flow in the EOS M280 PBF system, the build plate was divided into three sections (front, middle, and back as shown in Figure 1), with the expectation that any location dependence due to proximity to the cross flow should be discernable with this level of granularity. Simultaneously, the influence of printing orientation (i.e., X, Y, Z) on mechanical properties is of critical concern, given that the as-built microstructure has demonstrated anisotropy (Fulcher and Leigh, 2013). The build plan shown in Figure 2 illustrates the X, Y, and Z-oriented samples segregated into front, middle, and back sections. Each section contains 3 samples oriented in each direction (i.e., X, Y, Z) for both tensile and Charpy specimens, as well as an additional thin bar added for microstructural sampling. In Figure 2, these samples can be identified the axis with which they are aligned, with the Charpy blanks being larger than the tensile blanks. In total, each build produced 18 X/Y-oriented specimens and 9 Z-oriented specimens for each characterization method (i.e., tensile and Charpy). Z-oriented specimens were 'shielded' by a sacrificial part, in an effort to prevent it from being 'knocked over' by the recoater blade (see Section 4.2 for more discussion on this).
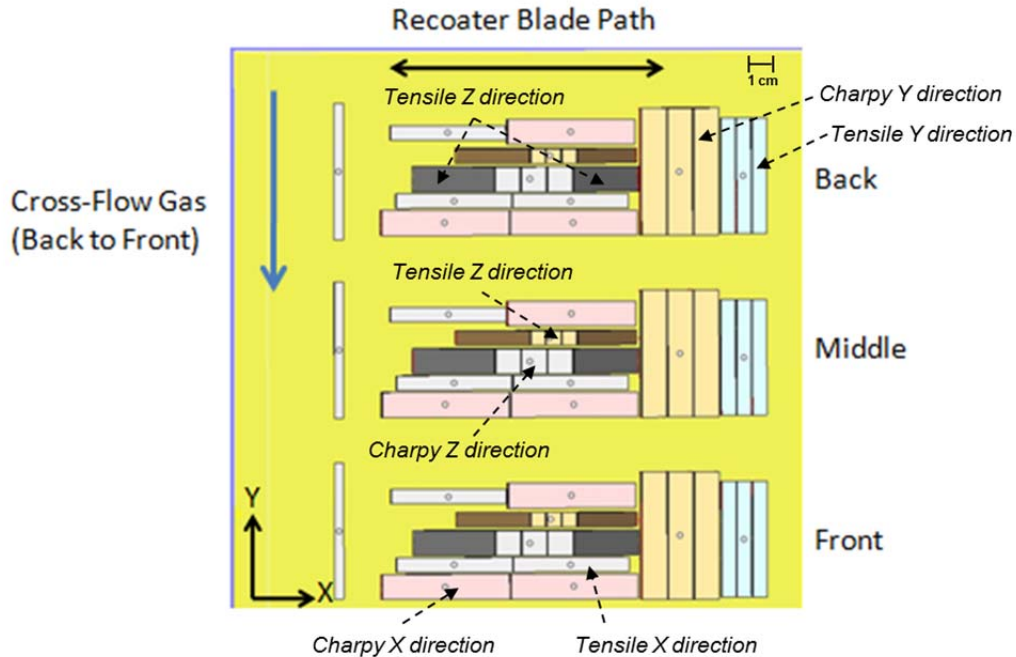
Figure 2: Overview of initial build plan from the perspective of the laser (top-down). Charpy (larger) and tensile (smaller) blanks are located in three sections to assess front-to-back variation due to cross-flow. This layout produces a build failure due to jamming of the recoater blade.

Any surfaces with an overhang greater than 45° are considered good candidate surfaces for support structures (Gibson et al, 2010), as printing over open spaces creates thin 'knife edges' which may crash the build or damage the recoater blade. Users will often rely on two types of support structures: (1) hatches and (2) pins. Hatched supports are typically algorithmically generated under overhanging surfaces, with a thin lattice formed from a single melt pool. The hatched lattice assists in holding down recently deposited regions which may distort or otherwise present a knife edge to the recoater blade. Pin supports are dense columns (or other geometries) which provide more substantial reinforcement than hatched regions due to a smaller surface area, with the drawback of being harder to remove after processing. Unlike hatches, pins are not generated algorithmically; they must be manually placed during the process design phase.

In our case, the simple geometry of a rectilinear block requires the entire bottom surface to be supported down to the build plate as a solid part. Direct contact between the build plate and a bottom surface may prevent distortion and unintended release of a part during the build; however, this approach is only applicable in the case of bulky or simple geometries, and it may not be adequate for more advanced designs that lack flat surfaces (e.g., organic shapes, lattice structures). Parts were not built directly onto the plate, despite the simple geometries used, as we sought to minimize the support material required for such simple geometries. Parts were offset from the build plate by 4 mm using support structures consisting of a square algorithmically generated mesh, as well as solid support pins, placed manually. These support pins were initially 0.5 mm in diameter at the contact point with the bars, but these were found to yield inadequate support, leading to the use of 1 mm support pins as discussed in Section 4.1. The locations of pins, as applied to the bottom of each section of parts are shown in Figure 3. As each pin must be placed manually, some variation among the pin locations can be seen.
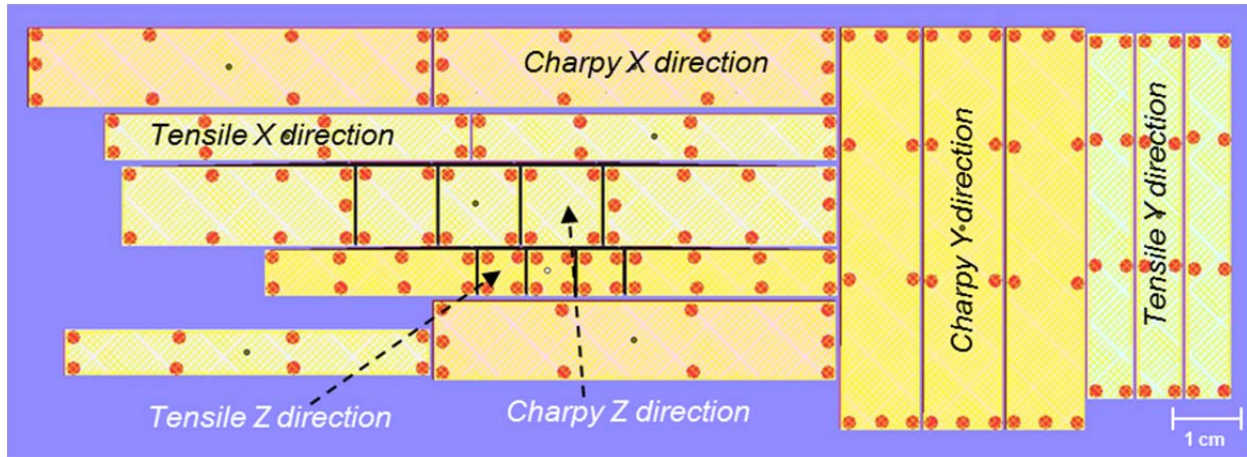
Figure 3: Support pin locations for each third of the initial build layout. Support pins are placed manually, and some variation in location from part to part is observed. Charpy samples are larger than tensile samples, having dimensions of (1.1 cm x 1.1 cm x 5.6 cm) and (0.6 cm x 0.6 cm x 5 cm) respectively.

3.3. Powder Feedstock

Many users of PBF systems like the EOS M280 are typically limited to using powders from the equipment manufacturer out of concern that they may be reducing part quality or voiding a machine warrantee by switching feedstock powder. There is strong interest in using powders from other manufacturers despite these concerns due to cost considerations and limited supplier base. This poses the question as to whether there is any variability in feedstock material and subsequently in material and microstructure properties arising from this change. Additionally, there is interest in this study in exploring whether the standard processing parameters for EOS Inconel 718 work well with comparable powders from other suppliers, or whether specific process parameters need to be developed for each powder from the different suppliers. For this study, 4 different Inconel 718 powders were obtained from three different suppliers, referred to hereafter as Suppliers A, B and C. Two powders with differing particle size were obtained from Supplier B. Costs ranged from $97/kg to $192/kg, and a comparison of the particle size, morphology, and material composition of each is discussed in Section 4.3.

3.4 Post-Processing and Mechanical Testing

After fabrication, stress relief of sample blanks was performed on some samples, to mitigate the impact of residual stress prior to removal of blanks from the build plate. Table 1 summarizes the conditions used for the three different powder supplies. For samples made with powder from Supplier A, plates were heated to $1750^{o}F\pm25^{o}F$ for 65 ± 10 minutes in a vacuum, with a subsequent air-assisted cooling. For samples made with powders from Suppliers B and C, a lower stress relief temperature, $1200^{o}F$ for 6 hours, was used to minimize any possible impact on the microstructure of the samples.

Table 1: Summary of Stress Relief Conditions

Powder Supplier	Temperature	Duration	Cooling
A	$1750^{o}F \pm 25^{o}F$	65 ± 10 min	Air
B	$1200^{o}F$	6 hrs	Air
C	$1200^{o}F$	6 hrs	Air

Blanks were removed from build plates using a submersed wire electrical discharge machining (EDM) process, prior to final machining and testing. Some samples were removed from the build plate without stress relief and tested for comparison. Machining and testing of specimens was performed by Westmoreland Mechanical Testing and Research (Youngstown, PA), applying ASTM specifications E23 and E8, to obtain Charpy and tensile data, respectively. The results of these tests are detailed next after discussing the manufacturing issues and problems that arose during the experiment.

4. Results and Discussion

4.1. Manufacturability Issues and Challenges

Contrary to common beliefs that additive manufacturing is as trivial as obtaining a 3D model and pressing a 'print' button to generate a part, the process of building the test specimens as designed and oriented in the build plan (see Figure 2) exposed several manufacturing issues that should be considered during the design and build phase. These issues can be grouped into two primary categories: (1) recoater blade and (2) support structures. As we discuss, careful consideration of these details can have a significant impact on the build success, and this learning is often not available or found in the literature—it is often learned by mistake and costly experience.

Recoater Blade Challenges

A recurring step in the building of each layer involves spreading a new layer of powder via a recoater blade in PBF systems. The EOS M280 uses a rigid blade that sweeps across the top of the previous layer while depositing the next layer of powder. While a variety of options (ceramic, carbon fiber, high-speed steel) are available for the recoater blade material, this work uses the high-speed steel blade. The initial build plan required several revisions and restarts due to the recoater blade jamming under certain build conditions. One of the conditions that causes frequent recoater blade jams is having too many surfaces parallel to the direction of blade travel. The forces generated as the blade sweeps across the previous surface of the part can often cause the blade to jam as it encounters edge regions which are distorting out of the build plane. The initial build plan suffered from having too many surface edges parallel to the blade (see Figure 2), increasing the contact area initially encountered by the blade and thus causing the front surface of the parts to jam the recoater blade as it attempted to pass over them. This caused two build failures and was addressed by rotating each part a few degrees in the XY plane (here, 5°), so that the recoater would only encounter a leading corner when passing over, rather than an entire edge.

Unfortunately, rotation of parts was not enough to avoid recoating issues. In addition to rotation of parts, parts nearest the powder supply platform (the first to encounter the recoater blade) were translated/offset by 0.1 mm as the group of lined leading corners has the similar effect of a 'leading edge' which can also catch the recoater blade. Applying a 0.2 mm offset in the X direction to each group of parts allowed the recoater blade to pass over the entire build without jamming. Figure 4 shows a successful build employing these rotations and offsets, as well as an initial simulated part layout, for contrast with the original build plan presented in Figure 2.
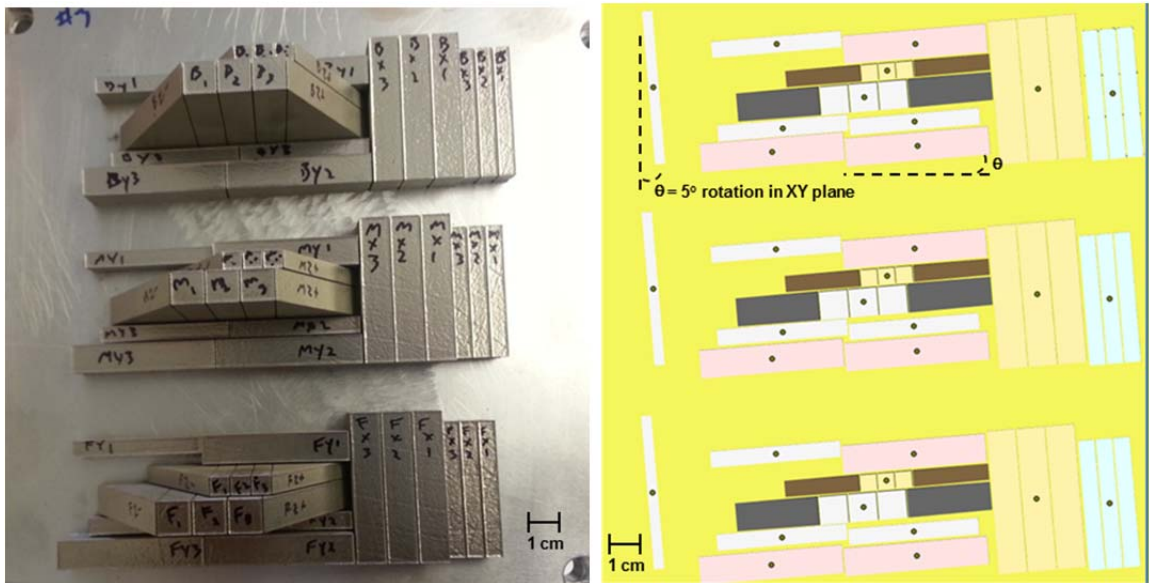

Figure 4: At left are as-built parts, with tilt and offsets applied. Sacrificial triangular 'shields' are on either side of the Z-oriented parts, in an effort to prevent the recoater blade from knocking them over. At right is a simulation of the final build design, with tilts applied to each part and offsets applied to the right-most parts.

Support Structure Challenges

In addition to the issues with the recoater, the support structure designs also proved to be an important manufacturability challenge. The need for adequate support structures in application of AM is critical, as under supported parts are prone to deformation and may promote build failures while over-supported parts require more post-build machining than might otherwise be required and undermine some of the primary justifications for using AM (minimal machining, reduced lead time, etc.). When designing support structures for an arbitrary geometry, there is theoretically a sweet spot where a minimum amount of support material may be employed while still obtaining a successful build. We endeavored to approach this ideal for the simple block geometries used.

An example of an under-supported and subsequently interrupted build is displayed in Figure 5, where the dense parts are seen to pull away from the support structures underneath due to the distortion caused by internal stresses. This is a function of both the support mesh and the solid support pins, neither of which were suitable for restraining the parts shown.
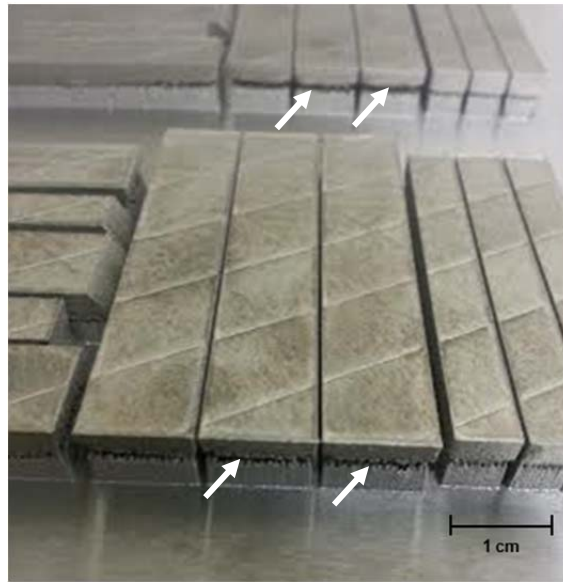
Figure 5: A failed build resulting from inadequate support structures. Arrows indicate the dark gap between the supports and the parts, indicating separation from the support structure. This build was terminated due to this issue.

Successful support structures were iteratively designed, and the difference between initial and adjusted support structure designs can be seen in Figure 6, where the upper supports represent the typical crosshatched mesh with 0.5 mm pins inserted which failed in Figure 5. This mesh exhibits 'teeth', providing a minimal contact area between the supports and the part. While these teeth are designed to facilitate support removal, they also limit the forces which the supports may apply to the as-built parts. Successful results were obtained using the support structures shown at the bottom of Figure 6, where 1 mm support pins were applied, and the mesh teeth were removed. This provided a larger surface area for contact between part and support, without increasing post-process machining substantially. It should be noted that the pin diameter was found to be the more critical modification, with the presence or absence of teeth making no difference to build success with 1 mm pins. We also note that the absence of teeth on the cross-hatched supports facilitates trapping of powder, which can otherwise fall through the gaps of toothed supports prior to stress relief or part removal.

Any user of PBF methods will need to develop their own support structure design methodology, which is expected to vary among use cases and may require modification for alternative material systems which exhibit more or less distortion during the course of the build (Calignano, 2014). This is expected to become a more critical design problem for contract manufacturers who are required to produce arbitrary geometries at low volumes, as opposed to a manufacturer whose large production runs may allow for optimized supports for a particular design. This is an ongoing and active area of investigation by many researchers.
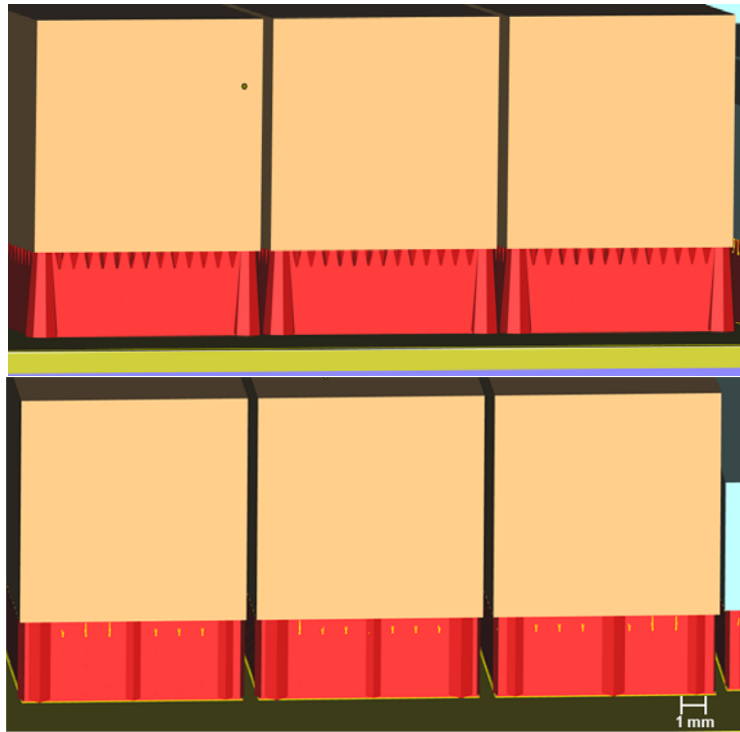
Figure 6: (top) Inadequate support structures with pins having a 0.5 mm diameter contact region with the part, resulting in the failure shown in Figure 5. (Bottom) Support structures with 1mm diameter pins where the teeth have been removed from the hatched support lattice.

4.2. Analysis of Build Plate Homogeneity

While there is some trial and error associated with part layout and support design, after finding a build layout with sufficient supports and suitable part orientation/position, successful builds were obtained consistently. The successful build shown previously in Figure 4 employs 5° of XY rotation and 0.2mm offsets along with strengthened support pins to prevent the recoater from jamming. Additionally, Z-oriented samples are 'shielded' by sacrificial triangular parts as shown in Figure 4, in an effort to prevent damage to them from the recoater blade.

Mechanical property measurements from stress-relieved samples from Supplier A are listed in Table 2 and Table 3, for Charpy and tensile test, respectively. We compare the differences arising from the blank location (front or back) and build plate orientation (X, Y and Z). While some variance in mechanical properties is observed across the entire build plate, any front-to-back variations are small in comparison to the variance caused by orientation.

Table 2: Room temperature (70°F) Charpy data for stress-relieved IN 718 from Supplier A

Sample ID	Energy (ft-lbs)	Mils Lateral Expansion	% Shear Fracture
X – Front	46	26	25
X – Back	47	20	20
Y – Front	45	22	25
Y – Back	46	24	20
Z – Front	56	31	30
Z – Back	54	31	30

Table 3: Room temperature (70°F) tensile data for stress-relieved IN 718 from Supplier A

Sample ID	UTS (ksi)	0.2% YS (ksi)	% Elong.	RA %	Modulus (Msi)
X – Front	166.8	110.4	28	42	29.1
X – Back	169.3	111.2	28	40	29.5
Y – Front	167.7	110.2	27	41	25.7
Y – Back	167.1	109.7	28	44	28.1
Z – Front	156.5	104.1	33	52	27.1
Z – Back	157.1	104.9	33	50	26.9

We can see from the data in Table 2 and Table 3 that the X- and Y-oriented samples all exhibit very similar mechanical properties whether they are from the front or the back of the build plate. The Z-oriented samples are not strongly influenced by part location on the build plate either; however, parts built in the Z-orientation exhibit substantially lower ultimate tensile strength and yield strength (~93-95%) compared to their X- and Y-oriented counterparts in the stress-relieved state. These anisotropy trends are as expected from comparable work, although our measured values differ slightly from other reported data due to the differences in stress-relief (Fulcher and Leigh, 2013).

Samples taken from a series of builds demonstrated that these mechanical property results were fairly consistent from run-to-run as guaranteed by EOS and reported elsewhere (e.g., Fulcher and Leigh, 2013); however, this does not account for long-term drift in the electro-mechanical systems of a single machine or the variation in product obtained from machine to machine. It may be expected that the subtle differences in design and operation among PBF manufacturers may yield additional variance from machine to machine as each manufacturer applies their own techniques for recoating, optimizing the beam/laser path, etc.
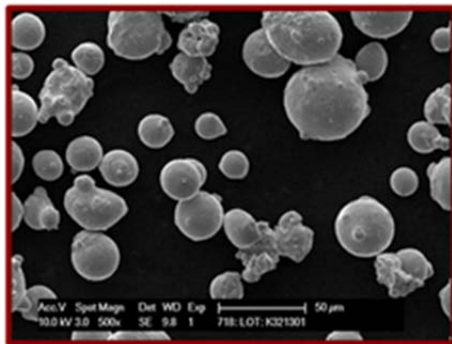
4.3. Characteristics of Alternative Powders

In 718 6A, a commonly used material in oil and gas applications, was obtained from 3 different suppliers. Two different powder sizes were obtained from Supplier B to examine the effect of mean particle size on mechanical properties. The material composition of the four IN 718 6A powders from the three suppliers used in this study are listed in Table 4. Particle size and distribution (see Table 5) were based on IN 718 powder feedstock provided by EOS. The powder feedstock from Suppliers A and C are comparable while the size and distribution of the feedstock from Supplier B is larger (Powder #1) and slightly smaller (Powder #2). This was
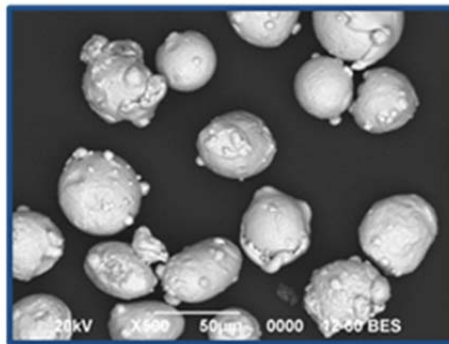
intentional to allow us to study the effect of having larger particle size feedstocks run at the same EOS process parameter settings. All powders are spherical in nature with minimal satellites as shown in scanning electron micrographs in Figure 7. Given the same elemental composition and powder morphology, the effects of the variance in particle size can be studied in the next section.

Table 4: Major elemental composition of IN 718 6A and powders from the three suppliers
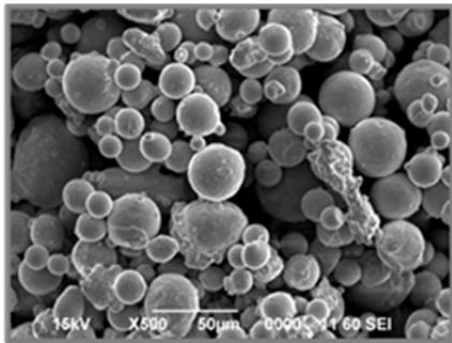
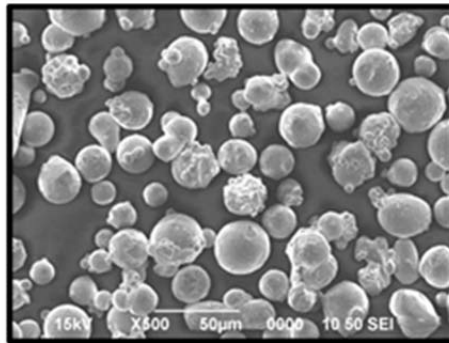| Element wt%	6A 718 Specification	Powder Supplier A	Powder Supplier B (Powder #1)	Powder Supplier B (Powder #2)	Powder Supplier C
Ni	50.0 − 55.0	50.0 − 55.0	53.26	53.09	53.4
Cr	17.0 − 21.0	17.0 − 21.0	18.97	19.03	18.7
Fe	Balance	Balance	18.05	17.78	Bal.
Nb	4.87 − 5.20	4.75 − 5.5	5.12	5.11	4.81
Mo	2.8 − 3.3	2.8 − 3.3	2.97	2.99	2.97
Ti	0.80 − 1.15	0.65 − 1.15	0.94	0.93	0.89
Al	0.40 − 0.60	0.2 − 0.8	0.53	0.51	0.49
Cu	< 0.23	< 0.3	0	0	0.09
C	< 0.045	< 0.08	0.04	0.04	0.03
Co	< 1.0	< 1.0	0.02	0.14	0.01

(a) Powder Supplier A

(b) Powder Supplier B (Powder #1)

(c) Powder Supplier B (Powder #2)

(d) Powder Supplier C

Figure 7: Scanning electron micrographs showing the spherical morphology of the powders from the three suppliers

Table 5: Powder characteristics by supplier

Supplier ID	Mean Particle Size (µm)	Standard Deviation (µm)
A	30.36	7.22
B – Powder #1	46.94	34.86
B – Powder #2	23.64	7.05
C	31.66	9.59

4.4. Analysis of Alternative Powders

After our initial studies on location-based variability and modifications of the builds based on manufacturing considerations with the powder from supplier A, several sets of samples were produced using the four powders in an effort to compare variability among those similar Inconel 718 powders currently available for use with PBF. The mechanical property results for these other powders are summarized in Table 6 and Table 7 along with desired specifications for Inconel 718 annealed and aged. Observations based on the data in the table follow.

Table 6: Comparison of mechanical properties in X/Y orientation by powder supplier

Supplier (Specimen State)	UTS (ksi)	0.2% YS (ksi)	% Elong.	RA %	Energy (ft-lbs)
A (stress relieved)	167.7	110.4	27.8	41.8	27.5
B – Powder #1 (as built)	157.6	114.8	29.3	43.3	-
B – Powder #1 (stress relieved)	158.0	115.0	29.0	41.8	-
B – Powder #2 (as built)	156.4	114.6	30.0	42.0	31.5
B – Powder #2 (stress relieved)	156.6	113.4	30.0	44.5	-
C (as built)	155.0	113.0	27.0	47.0	60.0
IN 718 Specs (Annealed & Aged) Minimum Values	150.0	120.0	20.0	35.0	35.0

Differences Between Powder Suppliers

The "as built" and "stress relieved" X/Y-oriented test samples from Suppliers B and C exhibit slightly lower ultimate tensile strength (UTS) compared to those from Supplier A, but all of the X/Y-oriented samples from all 3 suppliers exceed the desired UTS specification. The same is not true in the Z-orientation (see Table 7). The "as built" Z-oriented samples from Supplier A exceed the UTS specification and are even comparable to the X/Y-oriented samples from Supplier B, which is remarkable. The difference in the specimens from Supplier A are likely due to the differences in the stress relief conditions (see Table 1). The 0.2% yield strength

for "as built" and "stress relieved" samples from Suppliers B and C are slightly higher that of Supplier A, but they fall slightly below the desired specification, which is for a heat treated sample (annealed and aged). The 0.2% yield strength in the Z orientation is substantially lower for Suppliers A and C (see Table 7). The % elongation values are slightly higher for the samples from Supplier B's powders, but the specimens using Supplier A and Supplier C powders are comparable, and all of them exceed the desired specification. RA % values are comparable for Suppliers A and B in the "as built" and "stress relieved" states, and both are lower than from Supplier C. All of RA % values meet the specification in X/Y-oriented samples as well as the Z-oriented specimens (see Table 7). Only the samples made with powder feedstock from Supplier C meet the minimum specification for impact energy. As mentioned earlier, the specification listed in Table 6 is for solution annealed and aged Inconel 718. Thus, further optimized heat treatment is needed to improve the properties of DMLS Inconel 718.

Differences between As-Built and Stress-Relieved Parts

We see little to no differences in the mechanical properties of test specimens in these two states for a given powder supply. This is as expected, since we used a relatively low stress relief temperature for most of the samples, to avoid any effects on the microstructure and phase formations within the samples. The mechanical properties will likely improve with proper heat treatment and solution annealing.

Differences due to Particle Size

As seen in Table 5, average particle sizes and particle size distributions for powder feedstock from Supplier A and Supplier B (Powder #1) are nearly equivalent while Powder #1 from Supplier B has nearly twice the average particle size. Powder from Supplier C has the same average particle size, similar to Supplier B – Powder #2. We see no significant differences when comparing Powder #1 and Powder #2 from Supplier B, i.e., the larger average particle size does not appear to impact the mechanical properties in the "as built" or "stress relieved" states. Supplier C's "as built" specimens exhibit 112% of the tensile strength of Supplier A specimens and absorb 180% of the impact energy. It is possible that some of this variation is due to chemistry of the feedstock powders rather than variance in particle size distribution.

Table 7: Comparison of mechanical properties in Z orientation by powder supplier

Supplier (Specimen State)	UTS (ksi)	0.2% YS (ksi)	% Elong.	RA %	Energy (ft-lbs)
A (stress relieved)	156.8	104.5	33.0	51.0	33.5
C (as built)	141.0	90.0	34.0	54.0	67.0
IN 718 Spec (Annealed & Aged) Minimum Values	150.0	120.0	20.0	35.0	35.0

5. Summary and Future Work

In this work we have demonstrated the relative uniformity of parts produced throughout the build plate of a cross-flow equipped powder bed fusion system, and note that alternative powders may be used without retuning or alteration of processing parameters, provided that the particle size distribution, morphology, and nominal composition are consistent with the powder being exchanged. Build-to-build variations on the same machine with the same powder were not found to be substantially different with the caveat that long-term degradation, machine-to-machine variance, and manufacturer-to-manufacturer variance have not been explored in this study. It is expected that some performance variance will be exhibited in comparison to other PBF systems in that their methods for powder delivery, inert gas handling, and laser pathing are not shared among all equipment manufacturers. The extent to which these machine-to-machine variations influence the quality of the final product remains open for study, limited only by the relative expense of each system and the difficulty of controlling variables across platforms.

This study also illustrates that even commercially available metal AM systems have a significant learning curve with regard to design and execution of the build process, with particular concerns regarding the application of support structures to arbitrary geometries. For manufacturers focusing on a single product design, support optimization is still painful but worth the expense of getting it right. For contract manufacturers offering powder bed fusion capabilities in small lot sizes, significant problems remain in designing supports to obtain successful builds for arbitrary designs. While some design guidelines are beginning to be shared, lead user experiences are still relatively limited, and design rules have not yet been condensed into easily shared forms.

Acknowledgments

References

Bhavsar, R., A. Collins, S. Silverman, "Use of Alloy 718 and 725 in Oil and Gas Industry," published in Superalloys 718. 625. 706 and Various Derivatives, Edited by E.A. Loria, TMS (The Minerals. Metals & Materials Society), 2001.

Blackwell, P. L. "The mechanical and microstructural characteristics of laser-deposited IN718," *Journal of Materials Processing Technology*, vol. 170, no. 1–2, pp. 240–246, Dec. 2005.

Calignano, F., 2014, "Design Optimization of Supports for Overhanging Structures in Aluminum and Titanium Alloys by Selective Laser Melting," *Materials and Design*, 64, 203-213

DeBarbadillo, J. J. and S. K. Mannan, "Alloy 718 for Oilfield Applications," JOM, vol. 64, no. 2, pp. 265–270, Feb. 2012.

Ferrar, B., L. Mullen, E. Jones, R. Stamp, and C. J. Sutcliffe. "Gas flow effects on selective laser melting (SLM) manufacturing performance." Journal of Materials Processing Technology 212, no. 2 (2012): 355-364.

Frasier, W. E. "Metal Additive Manufacturing: A Review" Journal of Materials Engineering and Performance, Volume 23, Issue 6, pp 1917-1928, June 2014.

Fulcher, B. and D. K. Leigh, "Metals Additive Manufacturing Development at Harvest Technologies," Twenty Forth Annual International Solid Freeform Fabrication Symposium Proceedings, pp. 408-423, 2013.

Gao, W. Y. Zhang, D. Ramanuan, K. Ramani, Y. Chen, C. B. Williams, C.C.L. Wang, Y. C. Shin, S. Zhang, and P.D. Zavattieri, "The status, challenges, and future of additive manufacturing in engineering" Computer-Aided Design, April 2015.

Gibson, I., D. W. Rosen, and B. Stucker, Additive Manufacturing Technologies: Rapid Prototyping to Direct Digital Manufacturing, Springer, New York, NY, 2010.

Gratton, A. "Comparison of Mechanical, Metallurgical Properties of 17-4PH Stainless Steel between Direct Metal Laser Sintering (DMLS) and Traditional Manufacturing Methods," NCUR, 2012.

Jia, Q. and D. Gu, "Selective laser melting additive manufacturing of Inconel 718 superalloy parts: Densification, microstructure and properties," Journal of Alloys and Compounds, 2014.

Morton, P.A., Mireles, J. Mendoza, H., Cordero, P. M., Benedict, M., Wicker, R. B., "Enhancement of Low-Cycle Fatigue Performance from Tailored Microstructures Enabled by Electron Beam Melting Additive Manufacturing Technology", ASME Journal of Mechanical Design, 2015, in press.

Murr, L. E., Martinez, E., Amato, K. N., Gaytan, S. M., Hernandez, J., Ramirez, D. A., Shindo, P.W., Medina, F. and Wicker, R. B. "Fabrication of metal and alloy components by additive manufacturing: examples of 3D materials science." Journal of Materials Research and Technology 1, no. 1 (2012): 42-54.

Nassar, A.R., T. J. Spurgeon, and E.W. Reutzel, "Sensing defects during directed-energy additive manufacturing of metal parts using optical emissions spectroscopy," Solid Freeform Fabrication Symposium Proceedings. Austin, TX: University of Texas, 2014.

Schirra, J.J., R.H. Caless, R.W. Hatala, "The Effect of Laves Phase on the Mechanical Properties of Wrought and Cast +HIP Inconel 718," published in Superalloys 718. 625. 706 and Various Derivatives, Edited by E.A. Loria, TMS (The Minerals. Metals & Materials Society), 1991.

Scott-Emuakpur O., Schwartz J., George T., Holycross C., Cross C., and Slater J. (2015) Bending fatigue life characterization of direct metal laser sintering nickel alloy 718, Fatigue Fract Engng Mater Struct, doi: 10.1111/ffe.12286.

Spierings, A. B., N. Herres, and G. Levy. "Influence of the particle size distribution on surface quality and mechanical properties in AM steel parts." Rapid Prototyping Journal 17.3 (2011): 195-202.

Xiaoming Z., J. Chen, X. Lin, W. Huang, Study on microstructure and mechanical properties of laser rapid forming Inconel 718, Materials Science and Engineering: A, Volume 478, Issues 1–2, 15 April 2008, Pages 119-124.

Zhang, Y. N., X. Cao, and P. Wanjara. "Microstructure and hardness of fiber laser deposited Inconel 718 using filler wire." The International Journal of Advanced Manufacturing Technology 69, no. 9-12 (2013): 2569-2581.

Inconel is a registered trademark of the Special Metals Corporation.